Journal of Structural Geology, Vol. 15, No. 7, pp. 887 to 894, 1993
Printed in Great Britain

0191-8141/93 $06.00+0.00
Pergamon Press Ltd

Regional kinematics inferred from magnetic subfabrics in Archean rocks of Northern Ontario, Canada

GRAHAM J. BORRADAILE and JOHN F. DEHLS

Geology Department, Lakehead University, Thunder Bay, Ontario, Canada P7B 5E1

(*Received* 31 *March* 1992; *accepted in revised form* 31 *August* 1992)

Abstract—Strain analysis, observations of *L–S* fabrics and studies of the anisotropy of magnetic susceptibility (AMS) and of anisotropy of isothermal remanence (AIRM) reveal a sequence of progressive fabric development during regional deformation. *L–S* fabrics of quartz and feldspar grains are most transposed in regional transpression whereas the AMS subfabrics, controlled by the properties of late metamorphic silicates, record a later orientation of the ambient stress field. Anisotropy of magnetic remanence is caused by the still younger minerals, magnetite and pyrrhotite. Its anisotropy is less transposed than the AMS subfabric. Consequently the relative orientations of the three types of fabric yield a kinematic sequence of subfabrics developed during transpression. The *L–S* fabrics are most transposed, the AMS less transposed and the AIRM fabrics least transposed toward the plane of regional flattening. The results indicate that the deformation recorded by the three subfabrics was non-coaxial in the most general sense, with all three principal directions spinning with respect to the rocks during progressive straining.

INTRODUCTION

THE Archean rocks near Thunder Bay form part of the Superior Province of the Canadian Shield (Fig. 1). This province is divided lithologically (more recently supported by radiometric evidence) into successive E–W subprovinces sometimes termed 'belts' (Card & Cieselski 1986, Corfu & Stott 1986, Percival 1989). In this paper we examine the structural features of a sequence of greenschist facies metasedimentary rocks cropping out along the boundary of the Wabigoon and Quetico subprovinces. They include conglomerates and arkoses of littoral provenance, possibly deposited in alluvial fan and fluvial environments (Wood 1980). This sequence of rocks, termed the Seine River Group, occurs in a fault-bounded lozenge between the Quetico metasedimentary subprovince to the south and the Wabigoon greenstone–granitoid subprovince to the north (Figs. 1 and 2). The Seine River Group comprises immature feldspathic sandstones and polycyclic conglomerates which were derived from an already metamorphosed and schistose terrain. Clasts in the conglomerate include a variety of meta-granites, gneiss, vein-quartz, jasper, meta-basalt, rhyolite, fragments of older conglomerate and rare small fragments of possible quartzite. Regional considerations suggest this source was probably to the north.

The Seine Group is folded into a single phase of upright, very tight to isoclinal folds with vertical axial planes trending ENE–WSW (Jackson 1982). The hinges show gentle culminations and depressions of plunge so that the component of structural facing (Borradaile 1976) on their axial-plane schistosity is upwards, and steep to the east-northeast or west-southwest. The schistosity defines a strong *S* tectonite fabric (Flinn 1965) to the region and possesses an integral fabric lineation (*L*) defined by elongate clasts. *L* lies in the schistosity plane and plunges to the east-northeast. Later deformation is represented by an extremely feeble, erratically oriented crenulation cleavage as well as some minor faults and shear zones. These features are locally developed and rare: one would normally consider this region to have been affected by only one penetrative deformation phase.

Normally in NW Ontario the Archean strata have a vertical, E–W trend but occasionally the presence of a rigid major intrusion, such as the Bad Vermilion Complex in the present area, provides a strain shadow region in which the regional strain is reduced and into which deflections of the regional *L–S* fabrics are found (Fig. 2).

STRAIN ANALYSIS

The conglomerates and clastic rocks are suitable for the analysis of finite strain, which varies from very low strain (>30% shortening) adjacent to the Bad Vermilion Complex to 65% N–S shortening adjacent to Highway 11 and along the Seine River (Fig. 1). The strain was analysed by digitizing photographs and thin sections of plan-view sections of the rocks, and in some cases by other sections as well. The orientations and shapes of the digitized clast outlines were then analysed by a variety of methods using a program package developed for IBM compatible, personal computers using the methods explained by Borradaile (1987a). (This program is available by sending a formatted disk of either size in a pre-addressed mailer to G. Borradaile.)

The most productive methods were those of Robin (1977) and the harmonic mean estimator of Lisle (1977). The methods most suitable for the analysis of strain would require some allowance for the initial fabric (e.g. Dunnet & Siddans 1971, Lisle 1979); however the low angles between bedding and schistosity render this

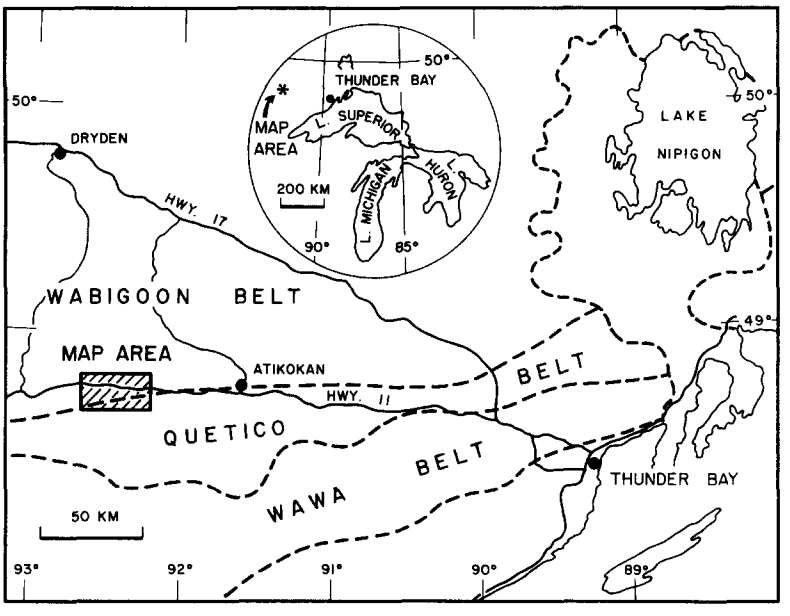

Fig. 1. Location of the area discussed, on the margins of the Quetico metasedimentary subprovince and Wabigoon greenstone subprovince in the Superior Province of the Canadian Shield.

approach unfeasible: see also Borradaile (1987a) for a discussion of this problem.

The results of the analyses on the conglomerate are listed in Table 1 and indicated on Fig. 2, giving the strain ellipse ratio in plan view as R_s.

MAGNETIC FABRICS

Traditional petrographic microfabric observations are slow and conventional strain analyses can be made only where suitable primary structures are available. However the anisotropy of rocks with respect to induced magnetization—the anisotropy of magnetic susceptibility (AMS)—is a means by which the microfabric anisotrophy of almost any homogeneous sample of a tectonite may be determined. The method has been known since the pioneering work of Graham (1954, 1966), but has only become competitive with conventional petrofabric or strain analysis since the advent of the personal computer. Recent work with AMS has shown that the ellipsoid defining the anisotropy is in most cases congruent with the finite strain ellipsoid (exceptions occur,

Table 1. Results of plan view strain analysis

Outcrop	Number of pebbles	Robin's method R_s	Robin's method % shortening	Harmonic mean R_s	Harmonic mean % shortening
1	116	2.71	39	2.72	39
2	186	2.84	41	2.94	42
3	105	8.59	66	7.66	64
4	156	8.08	65	7.46	63
5	61	5.91	59	5.51	57
6	184	4.23	51	4.09	51
7	201	3.68	48	3.68	48
8	106	7.36	63	6.92	62
9	221	4.20	51	5.43	57
10	243	4.23	51	4.45	53
11	228	4.47	53	4.72	54
12	123	1.90	27	2.16	32
13	41	1.63	22	1.91	28
14	70	2.01	29	2.25	33
15	125	1.91	28	2.16	32
16	154	5.70	58	5.24	56
17	163	8.38	65	7.33	63
18	122	2.80	40	2.88	41

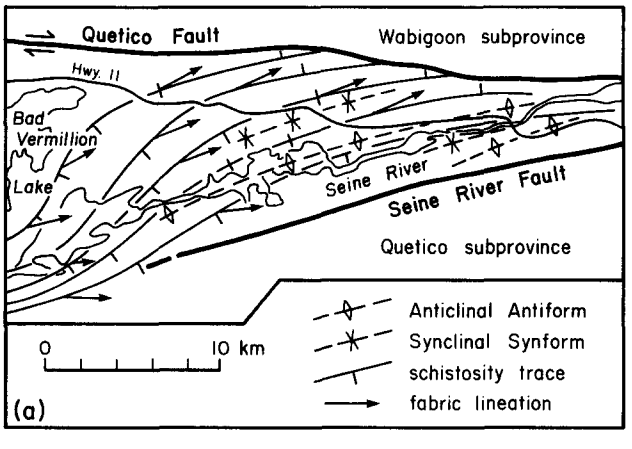

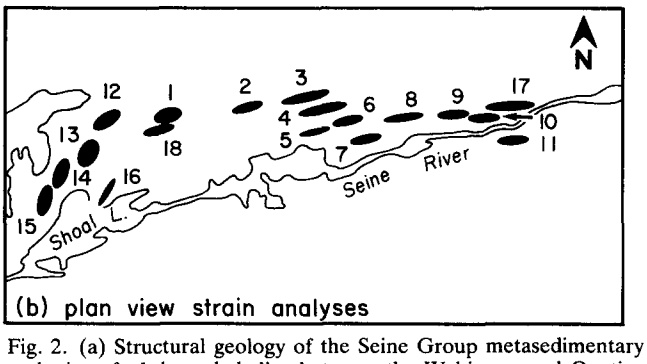

Fig. 2. (a) Structural geology of the Seine Group metasedimentary rocks in a fault-bounded slice between the Wabigoon and Quetico subprovinces. The Bad Vermilion pluton in the west of the area acts as a rigid body against which the Seine Group forms a strain shadow, shown here by the deflection of the S_1 schistosity. (b) The plan view, finite strain ellipses determined from clasts in the Seine conglomerates. Note the lower strains in the western part of the block adjacent to the Bad Vermilion pluton where a regional strain shadow occurs.

for example, where initial sedimentary fabrics are incompletely overprinted or where inverse fabrics are produced by special minerals; Potter & Stephenson 1988, Rochette 1989) but the ellipsoid is less eccentric than the strain ellipsoid (Hrouda 1982, MacDonald & Ellwood 1987, Borradaile 1988). The shape ratios of the ellipsoid do not simply relate to strain ratios because AMS is a summation of the induced magnetization contributions from a variety of paramagnetic silicates with transition metal cations; chlorite and biotite are common in this regard in this study. The AMS in these cases is controlled by the preferred crystallographic alignment of these minerals (Rochette & Vialon 1984, Henry 1989). Contributions are also commonly made by ferrimagnetic minerals, in this study magnetite and pyrrhotite. For magnetite the AMS contribution is controlled by the preferred shape orientation of the grains. For these reasons there is no simple relationship between the magnitudes of finite strain ratios and those of AMS (Borradaile & Mothersill 1984, Borradaile 1987b, 1991). The susceptibilities of metamorphic rocks derived from immature sediments and basic volcanic rocks, as in this region, are high (mean 2.73×10^{-3} SI on a volume basis) and can be measured with great precision (better than 1 part in 10^5).

Magnetic properties of the Seine Group Rocks

A variety of rock magnetic techniques have been applied to typical samples in order to ascertain their magnetic properties. The first of these, and the simplest, involves crushing samples to liberate grains. This procedure must be done carefully to avoid generating polymineralic fragments. A hand magnet is then passed over the separation to pick out the ferrimagnetic grains. In all our samples this yielded magnetite and a smaller amount of pyrrhotite. The remaining aggregate is then passed through a Franz magnetic separator several times at different field strengths and tilt angles. In this way each rock yielded five separate fractions of varying magnetic properties. The result of this simple procedure revealed that >75% of the low field susceptibility (and therefore of the AMS) is due to chlorite or biotite or both.

Susceptibility of metamorphic rocks is often due to paramagnetic silicates primarily, as confirmed in other studies (Coward & Whalley 1979, Rochette & Vialon 1984, Borradaile *et al.* 1985, 1987, Rochette 1987, Borradaile & Sarvas 1990). This can be checked simply by measuring the susceptibility at various temperatures. According to the Curie law a paramagnetic substance should show the following relation between susceptibility (k) and absolute temperature (T):

$$1/k = C(T - \theta),$$

where θ is a constant specific to the mineral. To avoid mineralogical alteration, a range of low temperatures is used by cooling the specimen to liquid nitrogen temperature (−196°C) and measuring its susceptibility as its temperature rises. Where θ is small the Curie relationship is approximately

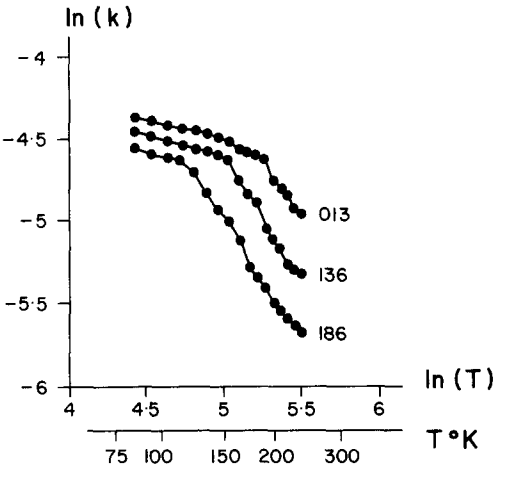

Fig. 3. Three typical samples of Seine sandstones show a decrease of low-field susceptibility with temperature (from liquid nitrogen to room temperature). The decay is compatible with the Curie law which suggests that the rocks predominantly behave as paramagnets. Thus the low-field magnetic susceptiblity (AMS) should chiefly correspond with the silicate fabrics in the rocks, rather than the iron oxide fabrics.

$$k \propto 1/T$$

and on a graph of $\ln(k)$ vs $\ln(T)$ the results should follow a slope of -1. Due to problems of thermal equilibration of the relatively large samples (10.5 cm^3), agreement with the law is poor, but the significant decrease in susceptibility with temperature leaves little doubt that the bulk susceptibility response is paramagnetic (Fig. 3).

Although the paramagnetic response dominates in our samples, the ferromagnetic traces are still valuable as these carry the remanent magnetisation of value to paleomagnetism. Also they possess another kind of anisotropy that we shall discuss later. To determine the presence and type of these minerals, the susceptibility of specimens has been measured while they have been heated in air from room temperature to 700°C and then as they cool to room temperature. In this way the changes in mineralogy produce characteristic susceptibility–temperature curves. Figure 4 illustrates

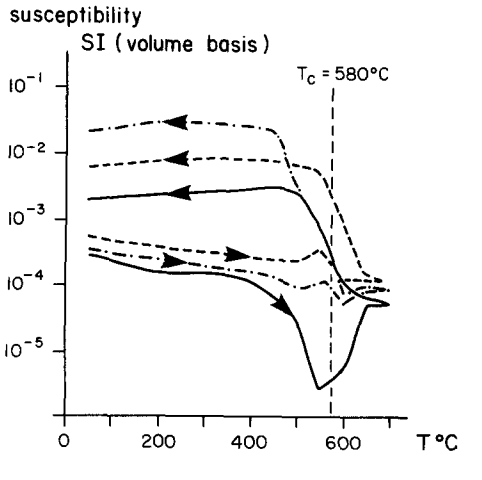

Fig. 4. The behaviour of low-field susceptibility with elevated temperature is shown for three typical samples of Seine sandstones. All three show notable decreases in susceptibility close to 580°C indicating the presence of magnetite. Two also show small 'Hopkinson peaks' (Dunlop 1974) just below the Curie point.

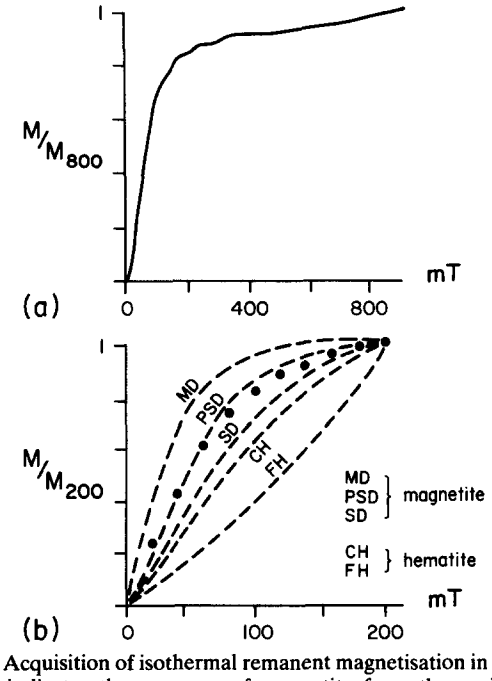

Fig. 5. Acquisition of isothermal remanent magnetisation in a typical sample indicates the presence of magnetite from the rapid initial increase in magnetization. The inability to achieve a plateau (a) suggests high coercivity weathering products are also present. Comparison with the standard curves of Dunlop (1971, 1973, 1981, 1983) indicates that the magnetite behaves as pseudo-single domain magnetite for the most part.

the results for some typical samples. All show little variation in susceptibility to about 400°C, then a steep drop to about 570°C, indicating the presence of magnetite. In two cases illustrated samples show a small peak below the Curie temperature—a 'Hopkinson peak' characteristic of the unblocking of remanence in magnetite (Dunlop 1974).

Curie balance tests were also run to determine the Curie temperatures. They yield slight evidence for a Curie point inflection at 320°C, indicative of pyrrhotite, and a significant Curie point minimum at about 570°C. The latter value is close to the value of 584°C for pure magnetite. Both of these minerals have been identified optically in the mineral separates used for Curie balance determinations. Finally, the acquisition of isothermal remanent magnetisation follows curves that can discriminate between different ferromagnetic traces. Figure 5 illustrates that the acquisition of IRM is typical for magnetite of multidomain to pseudo-single domain character.

ANISOTROPY OF MAGNETIC SUSCEPTIBILITY

AMS has been determined using a Sapphire Instruments SI-2 system operating at 750 Hz and an RMS field of 0.6 oersteds (79.6 A m^{-1}). Anisotropy was determined using 12 orientations for each specimen. AMS was determined before the specimens were exposed to any large magnetic fields so that the natural contributions of ferromagnetic components to the susceptibility were not changed (Potter & Stephenson 1990). The orientations of the maximum (k_{max}) and minimum (k_{min}) susceptibilities form well-defined groups for the region and compare well with the orientations of schistosity and fabric lineation (Fig. 6).

The shape of the AMS ellipsoid is best illustrated by the T parameter which varies from +1 for a perfect oblate ellipsoid to −1 for a perfect prolate ellipsoid (Jelinek 1981).

This parameter is more symmetrical than the Flinn parameter k usually used by structural geologists. It is defined by

$$T = \frac{\log_e F - \log_e L}{\log_e F + \log_e L}.$$

where $L = k_{max}/k_{int}$ and $F = k_{int}/k_{min}$, analogous to the Flinn parameters a and b for strain or fabric description.

The intensity of anisotropy or degree of eccentricity of the ellipsoid can be summarized in a single parameter P'

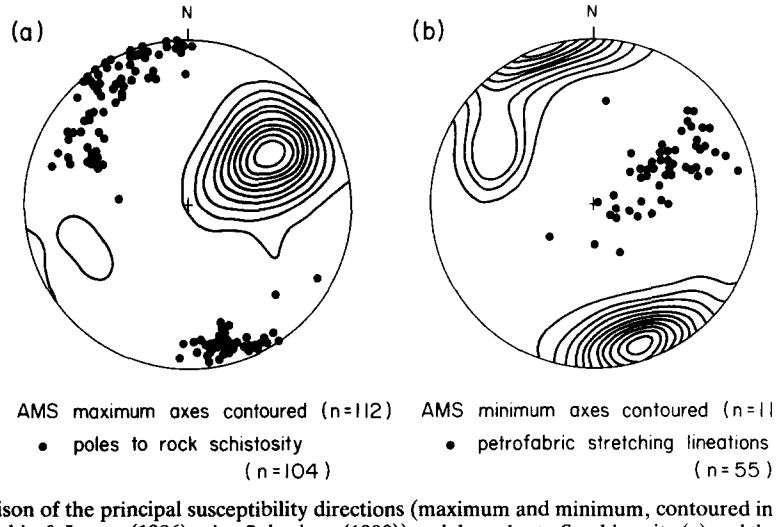

Fig. 6. Comparison of the principal susceptibility directions (maximum and minimum, contoured in a and b according to the method of Robin & Jowett (1986) using Spheristat (1990)) and the poles to S_1 schistosity (a) and the stretching lineations of clasts (b). The lowest contour represents a data density equal to that of an equal number of randomly distributed points. Higher contours show increases in density in steps equal to two-thirds of the expected density of randomly distributed data points.

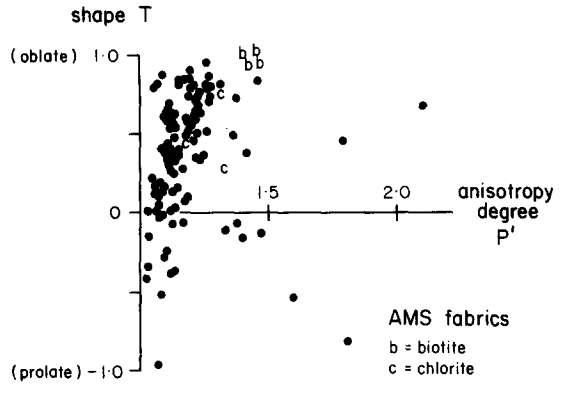

Fig. 7. Jelinek (1981) plot illustrating the anisotropy shape and intensity for the magnetic fabric ellipsoids defined by the anisotropy of low-field susceptibility (AMS). The anisotropies of typical metamorphic biotite and chlorite grains are shown from Borradaile *et al.* (1987).

(Jelinek 1981) which combines contributions from all three principal values. P' is defined as:

$$P' = \exp(\sqrt{(2((A_{max}^2 + A_{int}^2 + A_{min}^2)))},$$

where $A_{max} = (\log_e k_{max} - \log_e \bar{k})$, etc., and $\bar{k}$ = mean susceptibility. This is more convenient than the Flinn diagram approach which requires two parameters (a and b) for the same purpose. The Jelinek diagram (Fig. 7) indicates the range of anisotropies present. As expected they are dominantly in the flattened field, trending toward the intrinsic anisotropies of chlorite and biotite which are the mineral components chiefly dictating the AMS.

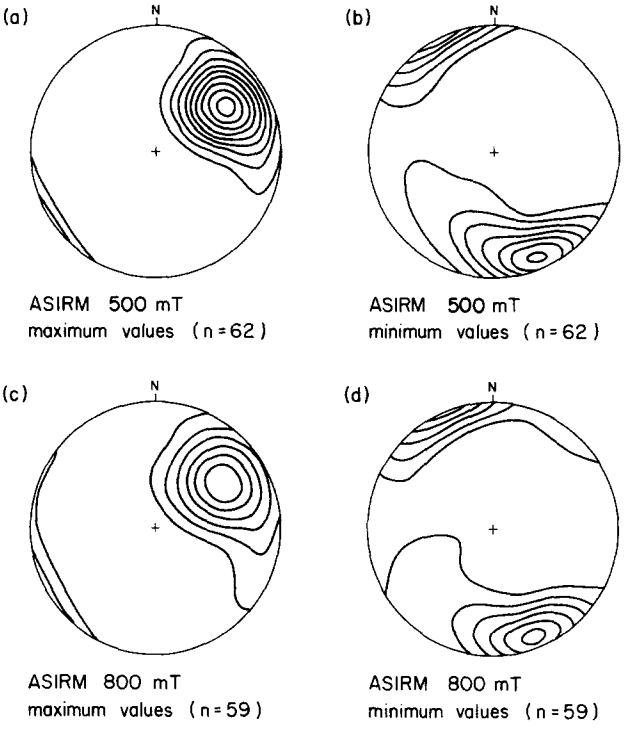

Fig. 8. Anisotropy of isothermal remanent magnetization (AIRM), reflecting the preferred orientations of magnetite for the most part. These are contoured by the method of Robin & Jowett (1986) using Spheristat (1990). They are presented for the anisotropies produced in two fields (600 and 800 mT), both of which saturate magnetite. The lowest contour represents a data density equal to that of an equal number of randomly distributed points. Higher contours show increases in density in steps equal to two-thirds of the expected density of randomly distributed data points.

ANISOTROPY OF ISOTHERMAL REMANENT MAGNETIZATION

It is possible to determine several types of magnetic anisotropy (Stephenson *et al.* 1986, Jackson 1991). Anisotropy of induced magnetization has been discussed above (AMS) but we may determine separately the anisotropy of the minerals which carry remanent magnetism; in this case magnetite and pyrrhotite. We chose to measure the simplest property in this regard; the anisotropy of the isothermal remanence. However, we determined the anisotropy of remanence acquired in high fields to be sure that the principal carriers of remanence were close to saturation when the remanence was applied in different directions whereas Daly & Zinsser (1973) used much lower fields for technical reasons. The procedure involves applying a strong magnetic field in a given direction and then measuring the remanent magnetization in a spinner magnetometer. This gives a measure of the maximum obtainable remanence in one direction. The procedure is repeated for several more directions in the specimen (a total of six directions was sufficient in the present study) and from these the ellipsoid describing the anisotropy of isothermal remanence (AIRM) was calculated. To ensure that the minerals were near to saturation remanence, this study was first performed using a magnetizing field of 500 mT (5000 oersteds). Then the study was repeated using a field of 800 mT. This confirmed the reproducibility of the results (Figs. 8 and 10). During the study, samples that could not be magnetized in the direction required by the appropriate step in the anisotropy procedure were discarded. About 15% of the samples fell into this category. If these specimens had been demagnetized between each stage of magnetization it is possible that they may also have yielded useful anisotropy results but this was not attempted.

The principal directions of AIRM are indicated in Fig. 9 for both levels of magnetization. These agree well, in a general sense, with the L–S and AMS fabrics (Fig. 6).

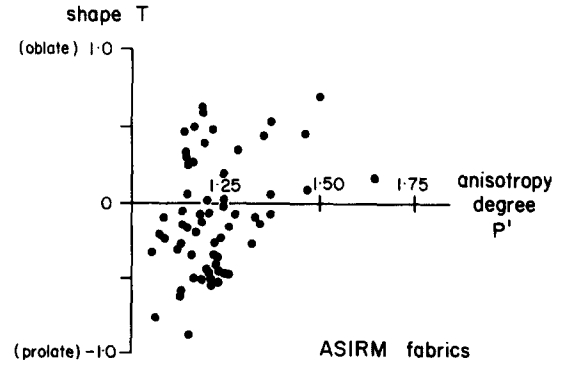

Fig. 9. A Jelinek (1981) plot showing the anisotropy shape and intensity for the magnetic fabrics defined by remanence; more precisely anisotropy of isothermal remanence (AIRM).

The intensities of the AIRM fabrics are slightly greater than those of the AMS fabrics (compare P' on Figs. 8 and 10). Moreover, the ellipsoid shapes are predominantly constricted, tending toward the prolate shape. This probably reflects the shape of multi-domain magnetite in these metamorphic rocks which is commonly slightly prolate. It contrasts with the AMS fabrics which lie in the field of flattened ellipsoids, reflecting the oblate symmetry of the crystal lattices of clorite and biotite from which the bulk of the AMS fabric arises. This highlights the danger of trying to infer magnitudes of strain from magnetic fabrics: magnetic fabrics primarily indicate the anisotropies (either lattice or dimensional) of the corresponding minerals and their relative proportions (Borradaile 1987b). However, it is not implied that prolate grains always give prolate magnetic fabrics and that oblate grains give oblate magnetic fabrics: the preferred orientation distribution of grains, the presence of single-domain magnetite, and the presence of minerals that give 'inverse fabrics' may complicate the resulting fabric (e.g. Potter & Stephenson 1988, Rochette 1989, Jackson 1991). Fabrics may differ also depending on the choice of magnetic property or technique for which the anisotropy is defined (Stephenson *et al.* 1987, Jackson 1991).

CONCLUSIONS

The presence of ENE–WSW-trending, tight upright folds and NNW–SSE shortened clastic fabrics presents a simple picture of a regional compression from the north-northwest. However, the subhorizontal or gently easterly plunging L component to the L–S fabrics indicates an along-strike extension, which is common in this region but difficult to reconcile with a simple, coaxial strain history which would require considerable extension parallel to the surface of the Earth. These features are more readily explained by a non-coaxial history involving regional shortening and synchronous shear, termed 'transpression' (Sanderson & Marchini 1984). That kinematic pattern would also account for the slight obliquity of the folds' axial traces with the belt boundaries, and the southwards flexure of the S–L fabrics as they are traced westwards into the strain shadow of the Bad Vermilion Complex (Fig. 2a). Such features have

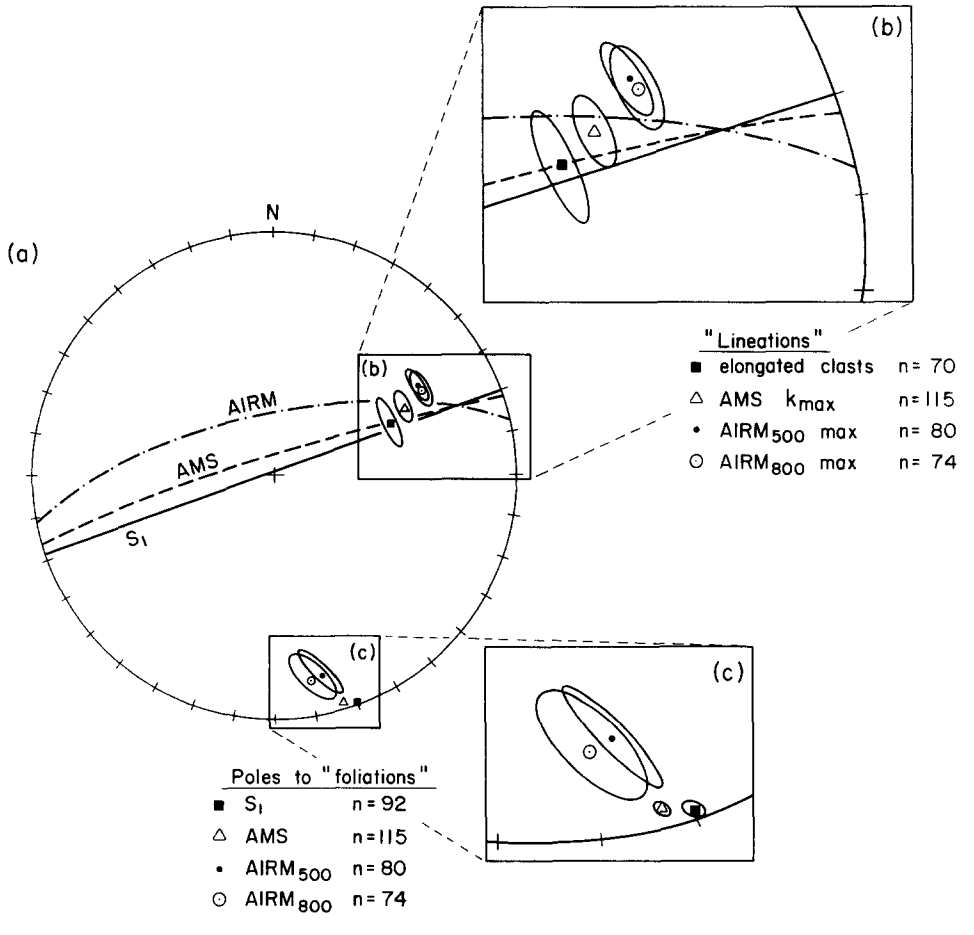

Fig. 10. Orientation data for the area east of the Bad Vermilion strain shadow. The mean orientations of the poles to the planar fabrics (schistosity, AMS fabric plane and fabric planes for AIRM at 500 and at 800 mT) and of the lineations for the fabrics (elongation of clastic grains, k_{max} of the AMS ellipsoid and the maximum elongation s of the ellipsoid for AIRM determined at 500 and 800 mT, respectively). The 95% confidence limits are shown as elliptical cones around these principal fabric directions as calculated by the program Spheristat (1990) according to the procedure of Hext (1963). The schistosity and clastic grain lineation (L–S fabric of Flinn 1965) are defined by deformed clasts of feldspar and quartz. The AMS ellipsoid is primarily controlled by the preferred crystallographic orientation of chlorite and biotite whereas the AIRM fabric is primarily controlled by the preferred shape orientation of multidomain magnetite.

been used elsewhere along the Quetico subprovince boundaries to document dextral transpression (Borradaile *et al.* 1988, Hudleston *et al.* 1988, Borradaile & Spark 1990) which appears to have dominated the later metamorphic–structural history of this region of NW Ontario.

Below we consider regional effects so that we have put aside the data from the strain shadow of the Bad Vermilion Complex. Here we consider only the data to the east of the strain shadow, where regional orientations of schistosity and grain elongation are found (Fig. 2).

The *S–L* fabrics defined by schistosity and distorted clasts indicates that the NNW shortening across the region is >55%, reducing to approximately 30% in the strain shadow of the Bad Vermilion Complex. The stretching lineation and schistosity define an $S > L$ fabric, described by a flat-shaped ellipsoid (Flinn 1965, Schwerdtner *et al.* 1977), compatible with the mean strain ellipsoids determined from shapes of flattened clasts. Magnetic fabrics, determined for low-field susceptibility (AMS) and for isothermal remanence (AIRM), also possess anisotropies that are defined by $S > L$ ellipsoids. Comparison of their shapes with the strain ellipsoid is not meaningful because each type of magnetic anisotropy sums the contributions from several minerals of varying abundance, each with its own preferred orientation distribution (Borradaile 1987b, 1988). However, the mean directions of the principal directions of each of the magnetic fabrics can be compared with the mean orientations of schistosity and mineral lineation. For simplicity we shall compare the orientations of minimum and of maximum principal directions of the ellipsoids. These are all similar in orientation but there are subtle and statistically significant differences at the 95% level. The lack of overlap of the 95% confidence limits about the principal directions indicate that the mean schistosity pole and the mean minima of magnetic susceptibility are distinctly inclined to one another (Fig. 10c). Similarly, the mean minimum direction of isothermal remanence is also inclined to the AMS and schistosity planes. (It may be noted that the two methods of determining the IRM anisotropy, at 500 and 800 mT yield directions whose 95% confidence limits overlap significantly, indicating the small influence of the strength of the magnetizing field under our conditions of AIRM measurement.) Inspection of the maximum directions of anisotropy (grain elongation, k_{max}, and IRM_{max}) indicate that these are also significantly different for the different subfabrics (Fig. 10b).

How may we interpret this? The *L–S* fabric sums the total strain history of the rock and this shows the most transposed fabric. The AMS fabric is dictated primarily by the preferred crystallographic orientation of chlorite and biotite which are relatively late metamorphic minerals, present for a shorter period of the rock's tectonic history. The AIRM fabrics, recorded by the magnetite (and to a minor extent by pyrrhotite), were present for a still shorter, later portion of the rock's tectonic history. Thus we can use the three fabrics as temporal indicators of acquisition of successive sub-fabrics in the rocks. The AIRM fabric records only the latest components; the AMS fabrics record a longer and older part of the tectonic deformation and the rock's *L–S* fabric defined by strained clasts summarizes the total transpressive history. The relative orientations of the mean values for these fabrics (Fig. 10) is consistent with progressive shortening in the N–S direction, first with 'overthrust' components of motion from the south, later from the north and dextral E–W shear throughout. During this process the extension directions recorded by successive fabric components gradually became less steep (Fig. 10b). These features of the kinematic history are summarized in cross-section in Fig. 11. However, the principal directions of shortening were not just spinning in one plane throughout the deformation. The deformation was non-coaxial in the most general sense, with all three principal directions changing orientation progressively in the tectonic sequence.

We suggest that the use of *L–S* fabrics combined with magnetic fabrics may provide regional indicators of tectonic kinematics elsewhere. *L–S* fabrics and AMS fabrics provide two rocks subfabrics which have been compared previously (Borradaile & Spark 1991). In this study, the sequence of rotations of the principal strains during deformation was further confirmed by another magnetic subfabric—the anisotropy of isothermal remanence (AIRM). However, the possibilities are by no means fully explored. Another type of magnetic remanence, anhysteretic remanent magnetization can also be applied to specimens to determine a difference aspect of remanence anisotropy (AARM). That technique may be more useful than AIRM because it can be applied to different subpopulations of remanence-carrying grains

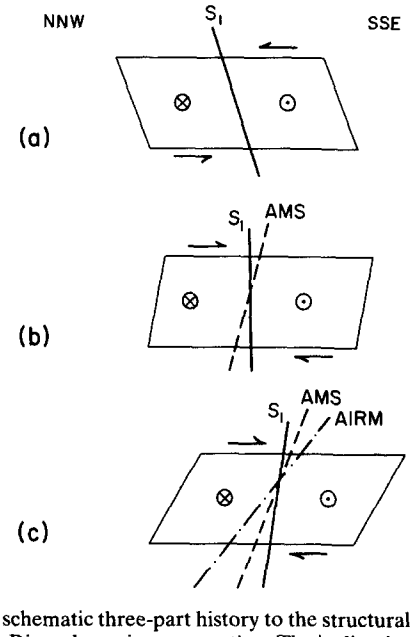

Fig. 11. A schematic three-part history to the structural development of the Seine River shown in cross-section. The inclinations of the fabric planes are slightly exaggerated for clarity. (a) Initial *S–L* fabric of clastic feldspar and quartz. (b) The planar component of the AMS fabric due to chlorite and biotite is superimposed. (c) The planar fabric of the ferromagnetic fabric (AIRM) of magnetite and pyrrhotite is added last. The sense of inferred 'overthrusting' is shown by half-arrows, and the regional component of dextral shear is shown by arrow-heads into and out of the plane of the section.

(magnetite in most cases) according to their coercivity (≈grain size) and has technical advantages as well (Jackson 1991). Thus it may be possible to define several anisotropic subfabrics of ARM from the different grain sizes (≈ages) of magnetite in a tectonite. This could provide many possibilities for studying the late kinematic history of tectonites.

Acknowledgements—We thank Mike Jackson (Minneapolis) for constructive criticism of this paper. This work was funded by NSERC grant A6861 to G. J. Borradaile. The rock physics facility in which the laboratory measurements were made was established at Lakehead University with funds from NSERC (Canada), BILD (Ontario), Bickell Foundation (Toronto), Noranda and American Barrick Resources. J. Dehls was an M.Sc. student at Lakehead for the duration of this study and was partially supported by a Lakehead Entrance Scholarship and a grant from the Centre for Northern Studies.

REFERENCES

Borradaile, G. J. 1976. Structural facing (Shackleton's rule) and the Paleozoic rocks of the Malaguide Complex near Véléz Rubio, SE Spain. *Proc. K. Ned. Akad. Wetenschappen* **79B**, 330–336.

Borradaile, G. J. 1987a. Analysis of strained sedimentary fabrics. *Can. J. Earth Sci.* **131**, 121–125.

Borradaile, G. J. 1987b. Anisotropy of magnetic susceptibility: rock composition versus strain. *Tectonophysics* **138**, 327–329.

Borradaile. G. J. 1988. Magnetic susceptibility, petrofabrics and strain. *Tectonophysics* **156**, 1–20.

Borradaile, G. J. 1991. Correlations of strain with anisotropy of magnetic susceptibility (AMS). *Pure & Appl. Geophys.* **135**, 15–29.

Borradaile, G. J., Keeler, W., Alford, C. & Sarvas, P. 1987. Anisotropy of magnetic susceptibility of some metamorphic minerals. *Phys. Earth & Planet. Interiors* **48**, 161–166.

Borradaile, G. J. & Mothersill, J. S. 1984. Coaxial deformed and magnetic fabrics without simply correlated magnitudes of principal values. *Phys. Earth & Planet. Interiors* **35**, 294–300.

Borradaile, G. J., Mothersill, J. S., Tarling, D. & Alford, C. 1985. Sources of magnetic susceptibility in a slate. *Earth Planet. Sci. Lett.* **76**, 336–340.

Borradaile, G. J. & Sarvas, P. 1990. Magnetic susceptibility fabrics in slates: structural, mineralogical and lithological influences. *Tectonophysics* **172**, 215–222.

Borradaile, G. J., Sarvas, P., Dutka, R., Stewart, R. & Stubley, M. 1988. Transpression in slates along the margin of an Archean gneiss belt, northern Ontario—magnetic fabrics and petrofabrics. *Can. J. Earth Sci.* **25**, 1069–1077.

Borradaile, G. J. & Spark, R. N. 1991. Deformation of the Archean Quetico-Shebandowan subprovince boundary in the Canadian Shield near Kashabowie, northern Ontario. *Can. J. Earth Sci.* **28**, 116–125.

Card, K. D. & Cieselski, A. 1986. Subdivisions of the Superior Province of the Canadian Shield. *Geosci. Can.* **13**, 5–13.

Corfu, F. & Stott, G. M. 1986. U–Pb ages for late magmatism and regional deformation in the Shebandowan belt, Superior province, Canada. *Can. J. Earth Sci.* **23**, 1075–1082.

Coward, M. P. & Whalley, J. S. 1979. Texture and fabric studies across the Kishorn Nappe, near Kyle of Lochalsh, Western Scotland. *J. Struct. Geol.* **1**, 259–273.

Daly, L. & Zinsser, H. 1973. Etude comparative des anisotropies de susceptibilité et d'aimantation isotherme. Conséquences pour l'analyse structurale et le paléomagnetisme. *Annales Géophys.* **29**, 189–200.

Dunlop, D. J. 1971. Magnetic properties of fine particle hematite. *Annales Géophys.* **27**, 269–293.

Dunlop, D. J. 1972. Magnetite: behaviour near the single-domain threshold. *Science* **176**, 41–43.

Dunlop, D. J. 1973. Superparamagnetic and single-domain threshold sizes in magnetite. *J. geophys. Res.* **78**, 1780–1793.

Dunlop, D. J. 1974. Thermal enhancement of magnetic susceptibility. *J. Geophys.* **40**, 439–451.

Dunlop, D. J. 1981. The rock magnetism of fine particles. *Phys. Earth & Planet. Interiors* **26**, 1–26.

Dunlop, D. J. 1983. Determination of domain structure in igneous rocks by alternating field and other methods. *Earth Planet. Sci. Lett.* **63**, 353–367.

Dunnet, D. & Siddans, A. W. B. 1971. Non-random sedimentary fabrics and their modification by strain. *Tectonophysics* **12**, 307–325.

Flinn, D. 1965. On the symmetry principle and the deformation ellipsoid. *Geol. Mag.* **102**, 36–45.

Graham, J. W. 1954. Magnetic susceptibility anisotropy, an unexploited petrofabric element. *Bull. geol. Soc. Am.* **65**, 1257–1258.

Graham, J. W. 1966. Significance of magnetic anisotropy in Appalachian sedimentary rocks. In: *The Earth Beneath the Continents* (edited by Steinhart, J. S. & Smith, T. J.). *Am. Geophys. Un. Geophys. Monogr.* **10**, 627–648.

Henry, B. 1989. Magnetic fabric and orientation tensor of minerals in rocks. *Tectonophysics* **165**, 21–27.

Hext, G. R. 1963. The estimation of second-order tensors, with related tests and designs. *Biometrika* **50**, 353–373.

Hudleston, P. J., Schultz-Ela, D. & Southwick, D. L. 1988. Transpression in an Archean greenstone belt, northern Minnesota. *Can. J. Earth Sci.* **25**, 1060–1068.

Hrouda, F. 1982. Magnetic anisotropy of rocks and its application in geology and geophysics. *Geophys. Surveys* **5**, 37–82.

Jackson, M. 1991. Anisotropy of magnetic remanence: a brief review of mineralogical sources, physical origins, and geological applications and comparison with susceptibility anisotropy. *Pure & Appl. Geophys.* **136**, 1–28.

Jackson, P. A. 1982. The structure, stratigraphy and strain history of the Seine Group and related rocks near Mine Centre, Northwestern Ontario. Unpublished M.Sc. thesis, Lakehead University.

Jelinek, V. 1981. Characterization of magnetic fabrics in rocks. *Tectonophysics* **79**, T63–T67.

Lisle, R. J. 1977. Estimation of the tectonic strain ratio from the mean shape of deformed elliptical markers. *Geologie Mijnb.* **56**, 140–144.

Lisle, R. J. 1979. Strain analysis using deformed pebbles: the influence of initial shape. *Tectonophysics* **60**, 263–277.

MacDonald, W. D. & Ellwood, B. B. 1987. Anisotropy of magnetic susceptibility: sedimentological, igneous, and structural–tectonic applications. *Rev. Geophys.* **25**, 905–909.

Percival, J. A. 1989. A regional perspective of the Quetico metasedimentary belt, Superior Province, Canada. *Can. J. Earth Sci.* **26**, 677–693.

Potter, D. K. & Stephenson, A. 1988. Single domain particles in rocks and magnetic fabric analysis. *Geophys. Res. Lett.* **15**, 1097–1100.

Potter, D. K. & Stephenson, A. 1990. Field-impressed anisotropies of magnetic susceptibility and remanence in minerals. *J. geophys. Res.* **95**, 15,573–15,588.

Robin, P.-Y. F. 1977. Determination of geological strain using randomly oriented strain markers of any shape. *Tectonophysics* **42**, T7–T16.

Robin, P.-Y. F. & Jowett, C. 1986. Computerized density contouring and statistical evaluation of orientation data using counting circles and continuous weighting functions. *Tectonophysics* **121**, 207–233.

Rochette, P. 1987. Magnetic susceptibility of the rock matrix related to magnetic fabric studies. *J. Struct. Geol.* **9**, 1015–1020.

Rochette, P. 1989. Susceptibility of matrix minerals and the ams–strain relationship. *Eos* **70**, 318.

Rochette, P. & Vialon, P. 1984. Development of planar and linear fabrics in Dauphinois shales and slates (French Alps) studied by magnetic anisotropy and its mineralogical control. *J. Struct. Geol.* **6**, 33–38.

Sanderson, D. J. & Marchini, W. R. D. 1984. Transpression. *J. Struct. Geol.* **6**, 449–458.

Schwerdtner, W. M., Bennett, P. J. & Janes, T. W. 1977. Application of *L–S* scheme to structural mapping and paleostrain analysis. *Can. J. Earth Sci.* **14**, 1021–1032.

Spheristat. 1990. Orientation analysis and plotting for MS-DOS computers. Version 1.0 & supplementary manual, 54 and 34 pp. respectively. Frontenac Wordsmiths, R.R. 5, Brockville, Ontario, Canada, K6V 5T5.

Stephenson, A., Sadikun, S. & Potter, D. K. 1986. A theoretical and experimental comparison of the anisotropies of magnetic susceptibility and remanence in rocks and minerals. *Geophys. J. R. astr. Soc.* **84**, 185–200.

Wood, J. 1980. Epiclastic sedimentation and stratigraphy in the North Spirit Lake and Rainy Lakes area: a comparison. *Precambrian Res.* **12**, 227–255.